

Identification of a gene signature closely related to immunosuppressive tumor microenvironment predicting prognosis of patients in EGFR mutant lung adenocarcinoma

Jia Li

Department of Integrated Chinese and Western Medicine, Affiliated Cancer Hospital of Zhengzhou University and Henan Cancer Hospital

Huahua Li

Department of Integrated Chinese and Western Medicine, Affiliated Cancer Hospital of Zhengzhou University and Henan Cancer Hospital

Chenyue Zhang

Department of Integrated Therapy, Fudan University Shanghai Cancer Center, Shanghai Medical College

Chenxing Zhang

Department of Nephrology, Shanghai Children's Medical Center, Shanghai Jiao Tong University School of Medicine

Haiyong Wang (✉ wanghaiyong6688@126.com)

Shandong Tumor Hospital and Institute

Research

Keywords: lung adenocarcinoma, mutation, gene signature, tumor microenvironment, tumor mutation burden

Posted Date: August 1st, 2020

DOI: <https://doi.org/10.21203/rs.3.rs-46728/v1>

License:  This work is licensed under a Creative Commons Attribution 4.0 International License.

[Read Full License](#)

Abstract

Background: Lung adenocarcinomas (LUAD) harboring epidermal growth factor receptor (EGFR) mutations generally are unable to benefit from immune checkpoint inhibitors (ICIs), due to an immunosuppressive tumor microenvironment (TME) and a lower tumor mutation burden (TMB). Currently, there has been no gene signature that can comprehensively evaluate the TME and predict the prognosis of EGFR mutant LUAD patients.

Methods: Using the cancer genome atlas (TCGA) database of EGFR mutant LUAD based on the immune score derived from the ESTIMATE algorithm, we screened the differential immune-related genes with prognostic value and compared the TMB profiles. Gene ontology (GO) and Kyoto encyclopedia of gene and genomic (KEGG) enrichment analysis were used to analyze the potential functions. The least absolute shrinkage and selection operator (LASSO) cox regression model was applied to identify a gene signature and constructed risk model. Kaplan-Meier survival and receiver operating characteristic (ROC) analysis were used to evaluate the prognostic value of the gene signature. CIBERSORT was used to evaluate the abundance of immune cells infiltration.

Results: We screened 396 the differential immune-related genes based on immune score, whose potential functions were significantly related to T cell differentiation, immune response, cell cycle and cell proliferation. The disparities of TMB profile could be found between the high and low immune score group. Then, we identified a three-gene signature, including B and T lymphocyte attenuator (BTLA), BUB1 mitotic checkpoint serine/threonine kinase B (BUB1B) and centromere protein E (CENPE). The three-gene signature could well identify at-risk patients of EGFR-mutant LUAD patients in the training and validating set, and the high-risk patients were related to shorter overall survival (OS) ($p=0.0053$ and $p=0.035$). The immune activity of B cells and macrophages were higher in the low-risk group, in contrast the immune activity of Natural Killer (NK) cells and T cells were higher in the high-risk group.

Conclusions: The three-gene signature closely related to immunosuppressive TME could predict risk prognosis of patients in EGFR mutant LUAD.

Background

Lung adenocarcinoma (LUAD) is one of the most common pathological types in non-small cell lung cancer (NSCLC), accounting for about half of all lung cancer cases [1]. In Western populations, epidermal growth factor receptor (EGFR) mutations are present in approximately 15% of LUAD, and even 50% in Asian populations [2-3]. EGFR-mutant LUAD patients showed a significant progression free survival (PFS) benefit with reduced side effects by treatment with tyrosine kinase inhibitors (TKIs). Although TKIs have been shown favorable clinical efficacy for advanced LUAD patients with sensitizing EGFR mutation, these patients eventually develop therapeutic resistance [4-6]. Recently, immunotherapy represented by immune-checkpoint inhibitors (ICIs) have impressively achieved success and anti-programmed cell death-1 (PD-1)/anti-programmed cell death ligand-1 (PD-L1) inhibitors have been approved by the United States

Food and Drug Administration (FDA) for the treatment of advanced NSCLC. However, EGFR-mutant NSCLC patients rarely derive a significant benefit from ICIs therapy [7-8].

Several studies have confirmed that EGFR mutations in NSCLC are closely related to an immunosuppressive tumor microenvironment (TME) [9-13] and a lower tumor mutation burden (TMB) [10,14-15], which cause an inferior response to PD-1 blockade in NSCLCs. EGFR mutations can lead to an uninfamed and immunosuppressive TME, with immunological tolerance, and weak immunogenicity [10,16]. In addition, the immunosuppressive TME may result from the absence of CD8+ T cell infiltrates and substantial reduction of TMB [9-10,16]. Emerging evidence demonstrates that EGFR mutations in NSCLC could affect a number of immune-related genes and induce an immunosuppressive TME [10,17-18]. Hence, it is of great importance to explore immune-related prognostic genes for identifying at-risk patients and revealing the status of the immunosuppressive TME.

The immune infiltrating cells and stromal cells are major cellular components of the TME [19]. The composition of infiltrating immune cells in TME not only play a critical role in progression and aggressiveness of cancer, but also have been proposed as an essential prognostic factor [20-21]. Assessing the status of immune infiltrating cells in TME will help more accurate diagnosis and prognostic evaluation of tumor patients. Currently, a variety of bioinformatics tools are used to predict the distribution of immune cells by analyzing specific gene signature [22-24]. In recent years, studies have shown that EGFR mutations may exert an anti-tumor immune response by affecting TME [9-13]. EGFR mutant LUAD patients have a unique TME, which may be different from wild-type EGFR patients. However, in EGFR-mutant LUAD patients, there has been no signature that can comprehensively evaluate the TME based on immune-related genes.

In this study, using EGFR mutations and mRNA data of LUAD from The Cancer Genome Atlas (TCGA), the differential immune-related genes with prognostic value were screened and the TMB profiles were compared based on different immune score groups. Then, Gene Ontology (GO) and Kyoto Encyclopedia of Gene and Genomic (KEGG) enrichment analysis were used to analyze the potential functions of the immune-related genes. Next, a three-gene signature closely related to immunosuppressive TME was identified and its potential prognostic value were further evaluated and validated. Finally, we explored the relationship between the signature and immune cells infiltration in the EGFR-mutated LUAD microenvironment.

Materials And Methods

Data source and processing

EGFR mutations and mRNA expression profiling data of 108 LUAD patients were downloaded from the GDC (<https://portal.gdc.cancer.gov/repository>). The TMB data of LUAD patients was obtained from the TCGA pan-cancer study (<https://gdc.cancer.gov/about-data/publications/panimmune>). Four datasets (GSE31210, GSE26939, GSE72094, and GSE11969), a total of 218 cases patients with EGFR mutations,

including 212 cases with clinical information were downloaded from the gene expression omnibus (GEO) database (<https://www.ncbi.nlm.nih.gov/geo/>).

ESTIMATE algorithm-derived immune scores

'Estimation of Stromal and Immune cells in Malignant Tumors using Expression data' (ESTIMATE) algorithm was used to calculate immune scores based on mRNA expression data. The algorithm could be downloaded from the Source Forge software repository (<https://sourceforge.net/projects/estimateproject/>) [24]. A single sample gene set enrichment analysis was used to generate three scores, of which stromal score indicated the presence of tumor matrix, immune score indicated tumor immune cell infiltration, and estimate score indicated tumor purity.

Screening for differential immune-related genes with prognostic value

Among 108 patients with lung adenocarcinoma EGFR positive, only 80 patients' immune scores were calculated according to mRNA expression data. Using multiples and t-test statistical methods, the differentially expressed genes (1769) were screened between the high and low immune score group. Data analysis was performed using packaging limma [25]. The cutoff value for screening differentially expressed genes were $|\log_2 \text{Fold Change}| > 1$ and p value < 0.05 . Univariate Cox regression was used to perform the prognosis of differentially expressed genes and the threshold was set to $p < 0.05$. 396 genes with significant prognostic value were eventually obtained among 1769 differentially expressed genes.

Enrichment analysis of immune-related genes with prognostic value

Database for Annotation, Visualization and Integrated Discovery (DAVID) was used to perform for GO functional and KEGG pathway enrichment analysis [26]. The cutoff value was False discovery rate (FDR) < 0.05 . We identified the GO categories through biological processes (BP), molecular functions (MF) and cellular components (CC).

Identification gene signature and construction risk model

Least Absolute Shrinkage and Selectionator Operator (LASSO) was a better high-dimensional regression classifier for selecting key genes affecting patient prognosis [27]. After multiple dimensionality reduction of prognostic genes using LASSO regression analysis, multiple genomes containing the optimal solution could be obtained. The LASSO regression analysis was performed using the publicly available R package.

The optimal prognostic model was constructed and a risk formula of risk score was used to evaluate the high-risk group and low-risk group. We obtained the score by the formula $\sum_i \omega_i \chi_i$, where ω_i and χ_i were the coefficient and expression value of each gene, respectively. The risk score for each sample was calculated according to the formula, and patients were divided into two groups based on the median risk score. In other words, the score was higher than the median risk score for the high-risk group, while the score was lower than the median risk score for the low-risk group.

Validation of the validity and reliability

Dataset GDC from TCGA was used as a training set to analyze the prognostic value of the risk model. Four external datasets (GSE31210, GSE26939, GSE72094, and GSE11969) were applied to verify the reliability of the risk model on the prognostic value. Univariate survival analysis of the risk model was used by R language ($p < 0.05$) [28]. Then we used survival receiver operating characteristic (ROC) curve to complete the area under the curve (AUC) of risk model [29].

Estimating the abundance of immune cells infiltration

We quantified the relative abundance of infiltrating immune cells within a complex gene expression mixture by platform CIBERSORT (<https://cibersort.stanford.edu/>) [30]. The abundance and composition of infiltrating immune cells in a sample could be obtained from gene expression data by CIBERSORT's deconvolution.

Result

Screening of differential immune-related genes with prognostic value

Among 80 patients with EGFR-mutated LUAD, the immune score could be calculated by immunocyte-related genes. Significant difference in immune score was observed between the high immune score group ($n=26$) and low immune score group ($n=54$) (Figure 1A, $p < 0.001$). Above the 80 patients with EGFR-mutated LUAD, 79 patients had complete clinical information (Table 1). Based on the mRNA expression profiles of 79 patients, the differentially expressed genes (1769) were screened between the high and low immune score group, of which 1050 genes were up-regulated and 719 genes were down-regulated (Figure 1B). Using univariate Cox regression, 396 genes with significant prognostic value were eventually obtained.

Table 1. The information of LUAD with EGFR positive status.

Clinical factors	The number of patients (n=79)
Sex	
Male	33
Female	46
AJCC stage	
Stage I	32
Stage II	22
Stage III	18
Stage IV	6
Survival status	
Alive	54
Dead	25
Age (median,year)	40-86 (70)
Overall Survival (median,month)	0.59-101.64 (18.17)

Comparison of TMB between the high and low immune score group

According to the TMB data of 80 patients, we assessed the TMB score of each patient, and compared the tumor mutation profile between the high and low immune score group. The result showed that TMB score of the low immune score group was higher than that of the high immune score group, in spite of the difference is not statistically significant ($p=0.07$). In Figure 1C, differences could be found in these mutant genes between the high and low immune score group, such as BOCRL1 (24% vs 6%), leucine rich repeat containing 7 (LRRC7) (19% vs 6%), family with sequence similarity 47 member C (FAM47C) (15% vs 2%), olfactory receptor family 5 subfamily F member 1 (OR5F1) (15% vs 6%), CUB and Sushi multiple domains 3 (CSMD3) (12% vs 24%), etc.

Enrichment analysis of differential immune-related genes with prognostic value

To explore the potential functions of 396 genes with prognostic value, we performed GO function and KEGG pathway enrichment analysis. The GO terminology for biological processes, molecular functions and cellular component terms were listed (Figure 2A, 2B and 2C). Top GO terms were significantly enriched in biological functions related to T cell differentiation, immune response, cell cycle and cell proliferation. In addition, pathway enrichment analysis of KEGG were mainly Cell cycle, Cell adhesion molecules and Cytokine-cytokine receptor interaction which were also related to the immune response(Figure 2D).

Identification gene signature and construction risk model

Among the 396 differential prognostic genes, the LASSO Cox regression model was applied to screen the most prognostic genes. We used a random sampling method of 10-cross validation to identify a three-

gene signature (BTLA, BUB1B and CENPE), which was closely related to immunosuppressive TME. Importantly, we found that the signature constructed by three genes was the most suitable prognostic model by confirmation and verification. Then, 80 patients were divided into the high risk group and low risk group according to the median risk score (Materials and Methods).

Evaluating the prognostic value of the gene signature

To further evaluate the prognostic value of the gene signature, Kaplan–Meier survival curves showed that patients in the high risk group had shorter overall survival (OS) than the low risk group (Figure 3A, $p=0.0053$). The risk score distribution, number of patients, distribution of patient survival time, and cumulative distribution of survival samples were also shown (Figure 3B–3E). Heat map of three gene expressions showed there were differences in the expression of three genes between high risk group and low risk group (Figure 3F).

Validating the validity and reliability of the gene signature

Four external datasets (GSE31210, GSE26939, GSE72094, and GSE11969), including 212 EGFR-mutated LUAD with clinical information, were used as a validating set. According to the median risk score of the three genes (BTLA, BUB1B and CENPE), 212 patients were divided into the high and low risk group (Materials and Methods). Figure 4A was a heat map of three gene expressions. The ROC curve was used to assess the prognostic value of the gene signature. As shown in Figure 4B, it can be found that the AUC of the gene signature at 12 months and 36 months was 0.8 and 0.7, respectively. Kaplan–Meier survival curves showed that patients of high risk group had shorter OS than these in the low risk group (Figure 4C, $p=0.035$). The above results indicated that our gene signature was feasible.

Estimating the abundance of immune cells infiltration

CIBERSORT was used to estimate the abundance of immune cells infiltration. The abundance of 24 types immune cells infiltration were normalized relative proportions in the high and low risk group (Figure 5A and 5B). The results showed that the immune activity of B cells and macrophages were higher in the low-risk group, in contrast the immune activity of NK cells and T cells were higher in the high-risk group.

Discussion

EGFR-mutant LUAD is an important molecular subtype that predicts high response rates to TKI therapy [4–6]. However, most clinical trials show that patients with EGFR mutations cannot benefit from immunotherapy [31–34]. The National Comprehensive Cancer Network (NCCN) guidelines do not recommend immunotherapy to patients with NSCLC harboring EGFR mutation at present [7–8]. Several mechanisms for poor responses to ICIs have been reported, such as a lower TMB and an uninflamed and immunosuppressive TME [9–16]. PD-1/PD-L1 axis may not be the main immune escape route in EGFR mutant lung cancer. EGFR activation is likely responsible for the uninflamed TME of this type tumor and participates in immunosuppression and immune escape [10, 17–18]. Therefore, better understanding the

TME and exploring immune-related prognostic biomarkers will help to reveal the molecular mechanism, identify at-risk groups of patients and improve the clinical outcome as well.

Firstly, we divided 80 patients with EGFR-mutated samples into high and low immune score group with different immune microenvironments. Then, we screened 396 the differential immune-related genes with prognostic value between the high and low immune score group. GO and KEGG enrichment analysis were used to analyze the potential functions of 396 immune-related genes with prognostic. Top GO terms were significantly enriched in biological functions related to T cell differentiation, immune response, cell cycle and cell proliferation. In addition, KEGG pathway enrichment analysis are mainly cell cycle, cell adhesion molecules and cytokine-cytokine receptor interaction. Therefore, the immune-related genes with prognostic value which were screened may reveal the status of the immunosuppressive TME.

TMB plays an important role in predicting tumor immunotherapy response [35–36] and immunosuppressive TME results to substantial reduction of the TMB in NSCLCs [10, 16]. We also compared the TMB profiles based on different immune score groups. TMB score of the low immune score group was higher than that of the high immune score group ($p = 0.07$) and differences could be found in these mutant genes between the high and low immune score group, such as BOCRL1 (24% vs 6%), LRRC7 (19% vs 6%), FAM47C (15% vs 2%), OR5F1 (15% vs 6%), CSMD3 (12% vs 24%), etc. EGFR mutant LUAD not only has a unique TME, but also has heterogeneity in the microenvironment. Based on the classification method of immune scores, we found that there are differences in TMB profiles in different immune score groups, which also means the difference in immune microenvironment status.

Many evidences demonstrate that EGFR mutations affect immune-related genes to exert a series of biological processes, such as immunosuppression, immune escape [37–39]. We identified 396 immune-related genes with prognostic, and constructed a three-gene (BTLA, BUB1B and CENPE) signature. Our three-gene signature can well divide EGFR-mutant LUAD patients in the training and validating set into high risk group and low risk group, and the high-risk patients were related to shorter OS. In addition, ROC curves confirm the robust prognostic value of the 3-gene signature in the training and validating set. The above finding confirmed that our TME-related three-gene signature had great and reliable prognostic value in EGFR-mutated lung adenocarcinoma patients.

Infiltrated immune cells, as an important part of TME, play an important role in the formation of TME [40–41]. Detailed characterization of immune infiltrating cells in TME will be more conducive accurate diagnosis and prognostic evaluation [20–21]. We evaluated the abundance of immune cells infiltration in the EGFR-mutated LUAD microenvironment. The immune activity of B cells and macrophages were higher in the low-risk group, in contrast the immune activity of NK cells and T cells were higher in the high-risk group. The above results confirm again that the three-gene signature is closely related to the TME and can provide a reference for immunotherapy response.

All three genes of our signature model have been proven to be related to the progress of tumor. BTLA is a recently discovered immunosuppressive receptor of the CD28 superfamily, in addition to CTLA-4 and PD-L1/PD-1 [42]. BTLA was mainly expressed in pulmonary carcinoma cells, but lowly expressed in tumor-

infiltrating lymphocytes (TILs). BTLA overexpression is a risk factor for the prognosis of NSCLC and that BTLA might be a novel therapeutic target for immunotherapy [43]. BUB1B plays a critical role in mitotic checkpoint signaling and chromosome congression, which is closely related to tumorigenesis [44–46]. BUB1B overexpression may serve as a predictive marker for lung adenocarcinoma and provide a new potential therapeutic target for inhibiting lung adenocarcinoma metastasis [47]. CENPE is an essential plus end-directed microtubule motor and acts to align chromosomes on the metaphase plate [48–49]. CENPE was highly expressed in NSCLC and the high expression of CENPE was related to the poorer prognosis of patients [50]. Although BUB1B and CENPE have not been reported to be involved in tumor immunity, their functions in tumor microenvironment are worthy of further study.

This study also has some limitations. Firstly, the study is only bioinformatics and retrospective research, and prospective clinical sample validation still needed. Secondly, the sample size of EGFR-mutated LUAD in our training set is small, and some samples still lack complete clinical information. We still need to expand the sample size or screen more databases to verify the accuracy and clinical value of the three-gene signature. Finally, lacking of data on EGFR-mutated LUAD patients treated with immune checkpoint inhibitors, we cannot determine the relationship between the signature and the response to immunotherapy.

Conclusions

We identified a three-gene signature based on immune scores, which had the robust prognostic value. More importantly, our signature may represent the status of TME for EGFR-mutant LUAD patients and demonstrated a closely association with TMB. Our study provided a novel insight into the prognostic stratification of patients with EGFR-mutated LUAD as well as provided in-depth understanding of the TME status for immunotherapy of EGFR-mutated LUAD.

Abbreviations

LUAD: lung adenocarcinomas; EGFR: epidermal growth factor receptor; ICIs: immune checkpoint inhibitors; TME: tumor microenvironment; TMB: tumor mutation burden; TCGA: the cancer genome atlas; ESTIMATE: Estimation of stromal and immune cells in malignant tumors using expression data; GO: gene ontology; KEGG: kyoto encyclopedia of gene and genomic; LASSO: least absolute shrinkage and selection operator; ROC: receiver operating characteristic; BTLA: B and T lymphocyte attenuator; BUB1B: BUB1 mitotic checkpoint serine/threonine kinase B; CENPE: centromere protein E; NK: Natural Killer; NSCLC: non-small cell lung cancer; PFS: progression free survival; TKI: tyrosine kinase inhibitors; PD-1: anti-programmed cell death-1 (PD-1); PD-L1: anti-programmed cell death ligand-1; FDA: food and drug administration; GEO: gene expression omnibus; DAVID: database for annotation, visualization and integrated discovery; FDR: false discovery rate; BP: biological processes (BP); MF: molecular functions; CC: cellular components; AUC: area under the curve; NCCN: national comprehensive cancer network.

Declarations

Ethics approval and consent to participate

This study was approved by the ethics committee of the Shandong Cancer Hospital affiliated to Shandong University and was consistent with the Helsinki Declaration. This study was mainly based on the GDC (<https://portal.gdc.cancer.gov/repository>) and the Gene Expression Omnibus datasets (GEO; GSE31210, GSE26939, GSE72094, and GSE11969) and personal privacy information was not involved, so the informed consent was not needed.

Consent for publication

All authors agree to publish.

Availability of data and material

We declared that materials described in the manuscript, including all relevant raw data, will be freely available to any scientist wishing to use them for non-commercial purposes, without breaching participant confidentiality.

Competing interests

All authors declare that there is no conflict of interest.

Funding

This study was supported jointly by Special funds for Taishan Scholars Project (Grant no. tsqn201812149), Academic promotion programme of Shandong First Medical University (2019RC004).

Authors' contributions

Haiyong Wang designed the project and proposed the idea; Huahua Li carried out data download and literature collection; Chenyue Zhang conducted bioinformatics analysis; Chenxing Zhang conducted chart and statistical processing; Jia Li wrote manuscript.

Acknowledgements

No.

References

1. Travis W D, Brambilla E, Noguchi M, et al. International Association for the Study of Lung Cancer/American Thoracic Society/European Respiratory Society: international multidisciplinary classification of lung adenocarcinoma: executive summary[J]. Proc Am Thorac Soc,2011,8(5):381-385.

2. Midha A, Dearden S, McCormack R. EGFR mutation incidence in non-small-cell lung cancer of adenocarcinoma histology: a systematic review and global map by ethnicity (mutMapII)[J]. *Am J Cancer Res*,2015,5(9):2892-2911.
3. Chan B A, Hughes B G. Targeted therapy for non-small cell lung cancer: current standards and the promise of the future[J]. *Transl Lung Cancer Res*,2015,4(1):36-54.
4. Maemondo M, Inoue A, Kobayashi K, et al. Gefitinib or chemotherapy for non-small-cell lung cancer with mutated EGFR[J]. *N Engl J Med*. 2010; 362 (25): 2380-2388.
5. Mitsudomi T, Morita S, Yatabe Y, et al. Gefitinib versus cisplatin plus docetaxel in patients with non-small-cell lung cancer harbouring mutations of the epidermal growth factor receptor (WJTOG3405): an open label, randomised phase 3 trial[J]. *Lancet Oncol* 2010; 11 (2): 121-128.
6. Zhou C, Wu YL, Chen G, et al. Erlotinib versus chemotherapy as first-line treatment for patients with advanced EGFR mutationpositive non-small-cell lung cancer (OPTIMAL, CTONG-0802): a multicentre, open-label, randomised, phase 3 study[J]. *Lancet Onc* 2011; 12 (8): 735-742.
7. Yamada T, Hirai S, Katayama Y, et al. Retrospective efficacy analysis of immune checkpoint inhibitors in patients with EGFR-mutated non-small cell lung cancer[J]. *Cancer Med*,2019,8(4):1521-1529.
8. Yu S, Liu D, Shen B, et al. Immunotherapy strategy of EGFR mutant lung cancer[J]. *Am J Cancer Res*,2018,8(10):2106-2115.
9. Gainor J F, Shaw A T, Sequist L V, et al. EGFR Mutations and ALK Rearrangements Are Associated with Low Response Rates to PD-1 Pathway Blockade in Non-Small Cell Lung Cancer: A Retrospective Analysis[J]. *Clin Cancer Res*,2016,22(18):4585-4593.
10. Dong Z Y, Zhang J T, Liu S Y, et al. EGFR mutation correlates with uninflamed phenotype and weak immunogenicity, causing impaired response to PD-1 blockade in non-small cell lung cancer[J]. *Oncoimmunology*,2017,6(11):e1356145.
11. Li H Y, Mcsharry M, Bullock B, et al. The Tumor Microenvironment Regulates Sensitivity of Murine Lung Tumors to PD-1/PD-L1 Antibody Blockade[J]. *Cancer Immunol Res*,2017,5(9):767-777.
12. Mascia F, Schloemann D T, Cataisson C, et al. Cell autonomous or systemic EGFR blockade alters the immune-environment in squamous cell carcinomas[J]. *Int J Cancer*,2016,139(11):2593-2597.
13. Lin A, Wei T, Meng H, et al. Role of the dynamic tumor microenvironment in controversies regarding immune checkpoint inhibitors for the treatment of non-small cell lung cancer (NSCLC) with EGFR mutations[J]. *Mol Cancer*,2019,18(1):139.
14. Spigel DR, Schrock AB, Fabrizio D, et al. Total mutation burden (TMB) in lung cancer (LC) and relationship with response to PD-1 / PD-L1 targeted therapies. *J Clin Oncol*. 2016; 34: 9017. https://doi.org/10.1200/JCO.2016.34.15_suppl.9017.
15. Jiao X D, He X, Qin B D, et al. The prognostic value of tumor mutation burden in EGFR-mutant advanced lung adenocarcinoma, an analysis based on cBioPortal data base[J]. *J Thorac Dis*,2019,11(11):4507-4515.

16. Santaniello A, Napolitano F, Servetto A, et al. Tumour Microenvironment and Immune Evasion in EGFR Addicted NSCLC: Hurdles and Possibilities[J]. *Cancers (Basel)*,2019,11(10).
17. Mansuet-Lupo A, Alifano M, Pecuchet N, et al. Intratumoral Immune Cell Densities Are Associated with Lung Adenocarcinoma Gene Alterations[J]. *Am J Respir Crit Care Med*,2016,194(11):1403-1412.
18. Gong Z, Chen J, Cheng J N, et al. Tumor Microenvironment Properties are Associated With Low CD68-positive Cell Infiltration and Favorable Disease-free Survival in EGFR-mutant Lung Adenocarcinoma[J]. *Clin Lung Cancer*,2018,19(5):e551-e558.
19. Chen Y P, Zhang Y, Lv J W, et al. Genomic Analysis of Tumor Microenvironment Immune Types across 14 Solid Cancer Types: Immunotherapeutic Implications[J]. *Theranostics*,2017,7(14):3585-3594.
20. Stankovic B, Bjørhovde H A K, Skarshaug R, et al. Immune Cell Composition in Human Non-small Cell Lung Cancer[J]. *Frontiers in Immunology*,2019,9.
21. Barnes T A, Amir E. HYPE or HOPE: the prognostic value of infiltrating immune cells in cancer[J]. *Br J Cancer*,2018,118(2):e5.
22. Galon J, Pagès F, Marincola FM, Angell HK, Thurin M, Lugli A, et al. Cancer classification using the Immunoscore: a worldwide task force. *J Transl Med.*(2012) 10:205.
23. Carter S L, Cibulskis K, Helman E, et al. Absolute quantification of somatic DNA alterations in human cancer[J]. *Nat Biotechnol*,2012,30(5):413-421.
24. Yoshihara K, Shahmoradgoli M, Martinez E, et al. Inferring tumour purity and stromal and immune cell admixture from expression data[J]. *Nat Commun*,2013,4:2612.
25. Ritchie M E, Phipson B, Wu D, et al. limma powers differential expression analyses for RNA-sequencing and microarray studies[J]. *Nucleic Acids Res*,2015,43(7):e47.
26. Huang D W, Sherman B T, Lempicki R A. Systematic and integrative analysis of large gene lists using DAVID bioinformatics resources[J]. *Nat Protoc*,2009,4(1):44-57.
27. Tibshirani R. The lasso method for variable selection in the Cox model[J]. *Stat Med*,1997,16(4):385-395.
28. O'Quigley J, Moreau T. Cox's regression model: computing a goodness of fit statistic[J]. *Comput Methods Programs Biomed*,1986,22(3):253-256.
29. Heagerty P J, Lumley T, Pepe M S. Time-dependent ROC curves for censored survival data and a diagnostic marker[J]. *Biometrics*,2000,56(2):337-344.
30. Chen B, Khodadoust M S, Liu C L, et al. Profiling Tumor Infiltrating Immune Cells with CIBERSORT[J]. *Methods Mol Biol*,2018,1711:243-259.
31. Herbst R S, Baas P, Kim D W, et al. Pembrolizumab versus docetaxel for previously treated, PD-L1-positive, advanced non-small-cell lung cancer (KEYNOTE-010): a randomised controlled trial[J]. *Lancet*,2016,387(10027):1540-1550.
32. Borghaei H, Paz-Ares L, Horn L, et al. Nivolumab versus Docetaxel in Advanced Nonsquamous Non-Small-Cell Lung Cancer[J]. *N Engl J Med*,2015,373(17):1627-1639.

33. Rittmeyer A, Barlesi F, Waterkamp D, et al. Atezolizumab versus docetaxel in patients with previously treated non-small-cell lung cancer (OAK): a phase 3, open-label, multicentre randomised controlled trial[J]. *Lancet*,2017,389(10066):255-265.
34. Lee C K, Man J, Lord S, et al. Checkpoint Inhibitors in Metastatic EGFR-Mutated Non-Small Cell Lung Cancer-A Meta-Analysis[J]. *J Thorac Oncol*,2017,12(2):403-407.
35. Rizvi N A, Hellmann M D, Snyder A, et al. Cancer immunology. Mutational landscape determines sensitivity to PD-1 blockade in non-small cell lung cancer[J]. *Science*,2015,348(6230):124-128.
36. Hellmann M D, Nathanson T, Rizvi H, et al. Genomic Features of Response to Combination Immunotherapy in Patients with Advanced Non-Small-Cell Lung Cancer[J]. *Cancer Cell*,2018,33(5):843-852.
37. Zaiss D M, van Loosdregt J, Gorlani A, et al. Amphiregulin enhances regulatory T cell-suppressive function via the epidermal growth factor receptor[J]. *Immunity*,2013,38(2):275-284.
38. Wang S, Zhang Y, Wang Y, et al. Amphiregulin Confers Regulatory T Cell Suppressive Function and Tumor Invasion via the EGFR/GSK-3beta/Foxp3 Axis[J]. *J Biol Chem*,2016,291(40):21085-21095.
39. Park S J, Nakagawa T, Kitamura H, et al. IL-6 regulates in vivo dendritic cell differentiation through STAT3 activation[J]. *J Immunol*,2004,173(6):3844-3854.
40. Binnewies M, Roberts EW, Kersten K, Chan V, Fearon DF, Merad M, Coussens LM, Gaborilovich DI, Ostrand-Rosenberg S, Hedrick CC, et al: Understanding the tumor immune microenvironment (TIME) for effective therapy. *Nat Med* 24: 541-550, 2018.
41. Roma-Rodrigues C, Mendes R, Baptista P V, et al. Targeting Tumor Microenvironment for Cancer Therapy[J]. *Int J Mol Sci*,2019,20(4).
42. Karakatsanis S, Bertsiadis G, Roussou P, et al. Programmed death 1 and B and T lymphocyte attenuator immunoreceptors and their association with malignant T-lymphoproliferative disorders: brief review[J]. *Hematol Oncol*,2014,32(3):113-119.
43. Li X, Xu Z, Cui G, et al. BTLA Expression in Stage I-III Non-Small-Cell Lung Cancer and Its Correlation with PD-1/PD-L1 and Clinical Outcomes[J]. *Onco Targets Ther*,2020,13:215-224.
44. Bolanos-Garcia V M, Blundell T L. BUB1 and BUBR1: multifaceted kinases of the cell cycle[J]. *Trends Biochem Sci*,2011,36(3):141-150.
45. Elowe S. Bub1 and BubR1: at the interface between chromosome attachment and the spindle checkpoint[J]. *Mol Cell Biol*,2011,31(15):3085-3093.
46. Karess R E, Wassmann K, Rahmani Z. New insights into the role of BubR1 in mitosis and beyond[J]. *Int Rev Cell Mol Biol*,2013,306:223-273.
47. Chen H, Lee J, Kljavin N M, et al. Requirement for BUB1B/BUBR1 in tumor progression of lung adenocarcinoma[J]. *Genes Cancer*,2015,6(3-4):106-118.
48. Hirokawa N, Noda Y, Tanaka Y, et al. Kinesin superfamily motor proteins and intracellular transport[J]. *Nat Rev Mol Cell Biol*,2009,10(10):682-696.

49. Kapoor T M, Lampson M A, Hergert P, et al. Chromosomes can congress to the metaphase plate before biorientation[J]. *Science*,2006,311(5759):388-391.
50. Hao X, Qu T. Expression of CENPE and its Prognostic Role in Non-small Cell Lung Cancer[J]. *Open Med (Wars)*,2019,14:497-502.

Figures

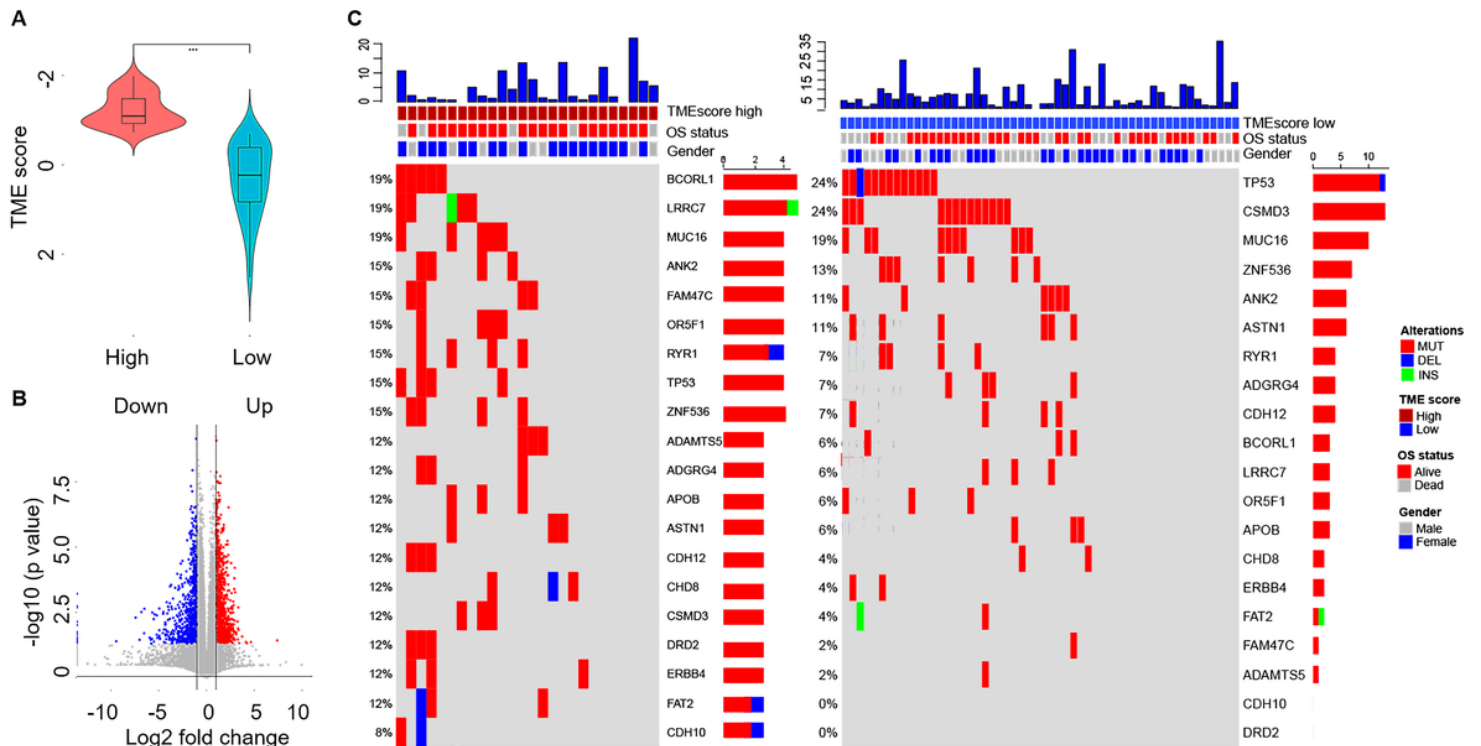


Figure 1

Screening of differential immune-related genes and comparison of tumor mutation burden (TMB) between the high and low immune score group. (A) Comparison of tumor microenvironment (TME) immune scores between the high and low immune score group. (B) Screening of differential immune-related genes between the high and low immune score group. Red represents up-regulated genes; blue represents down-regulated genes. (C) comparison of tumor mutation burden (TMB) score, overall survival status, gender and mutant genes alterations between the high and low immune score group.

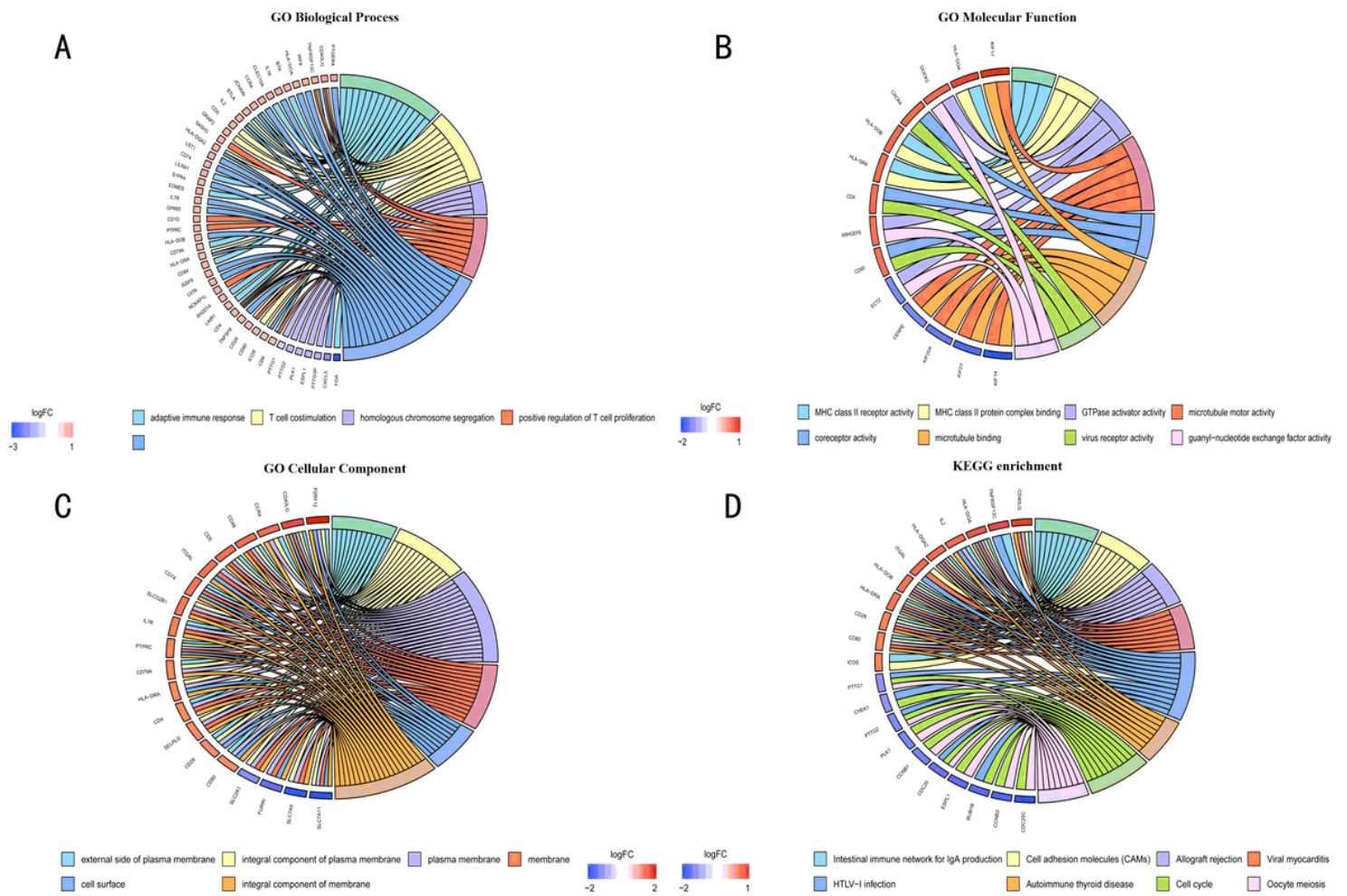


Figure 2

Enrichment analysis of differential immune-related genes with prognostic value. The gene ontology (GO) terminology for biological processes (A), molecular functions (B) and cellular component terms (C). (D) KEGG pathway enrichment analysis.

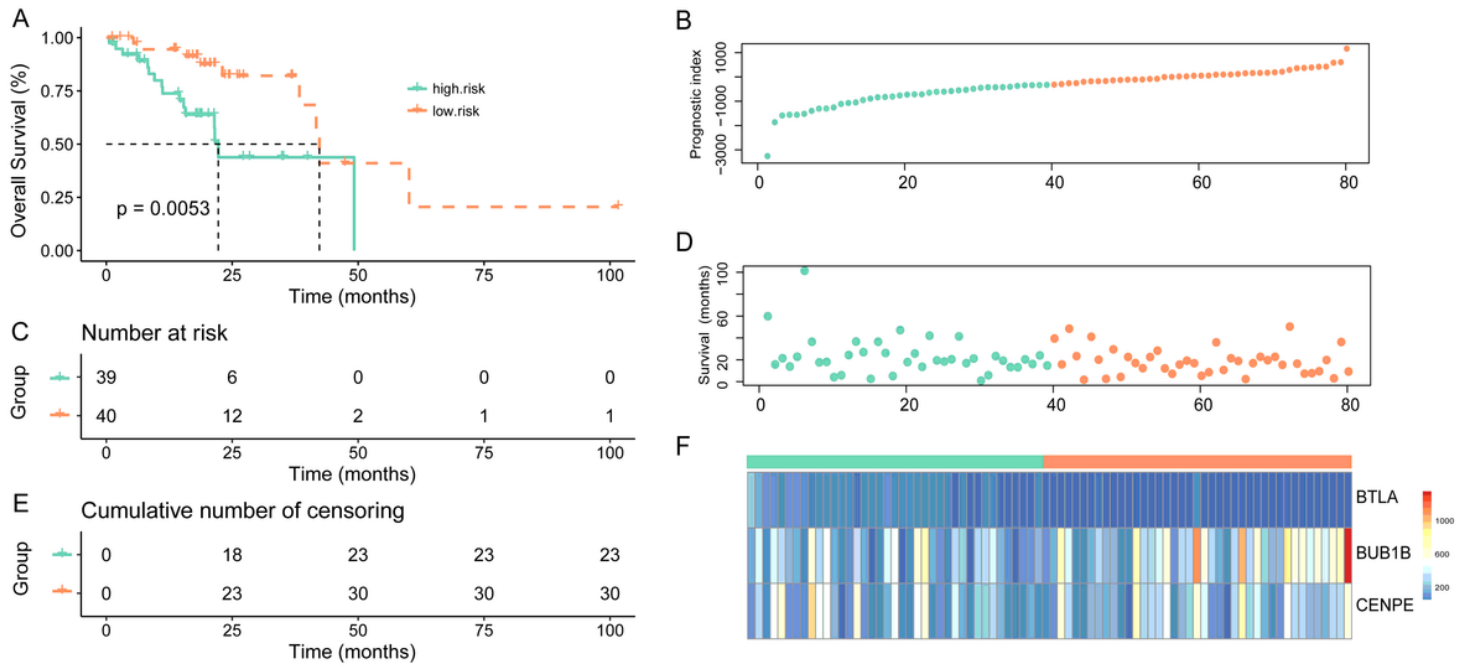


Figure 3

Evaluating the prognostic value of the gene signature in dataset GDC from TCGA. (A) Kaplan–Meier survival curves for overall survival (OS) in the high and low risk group. The risk score distribution (B), number of patients (C), distribution of patient survival time (D), and cumulative distribution of survival samples (E). (F) Heat map of three gene expressions (BTLA, BUB1B and CENPE).

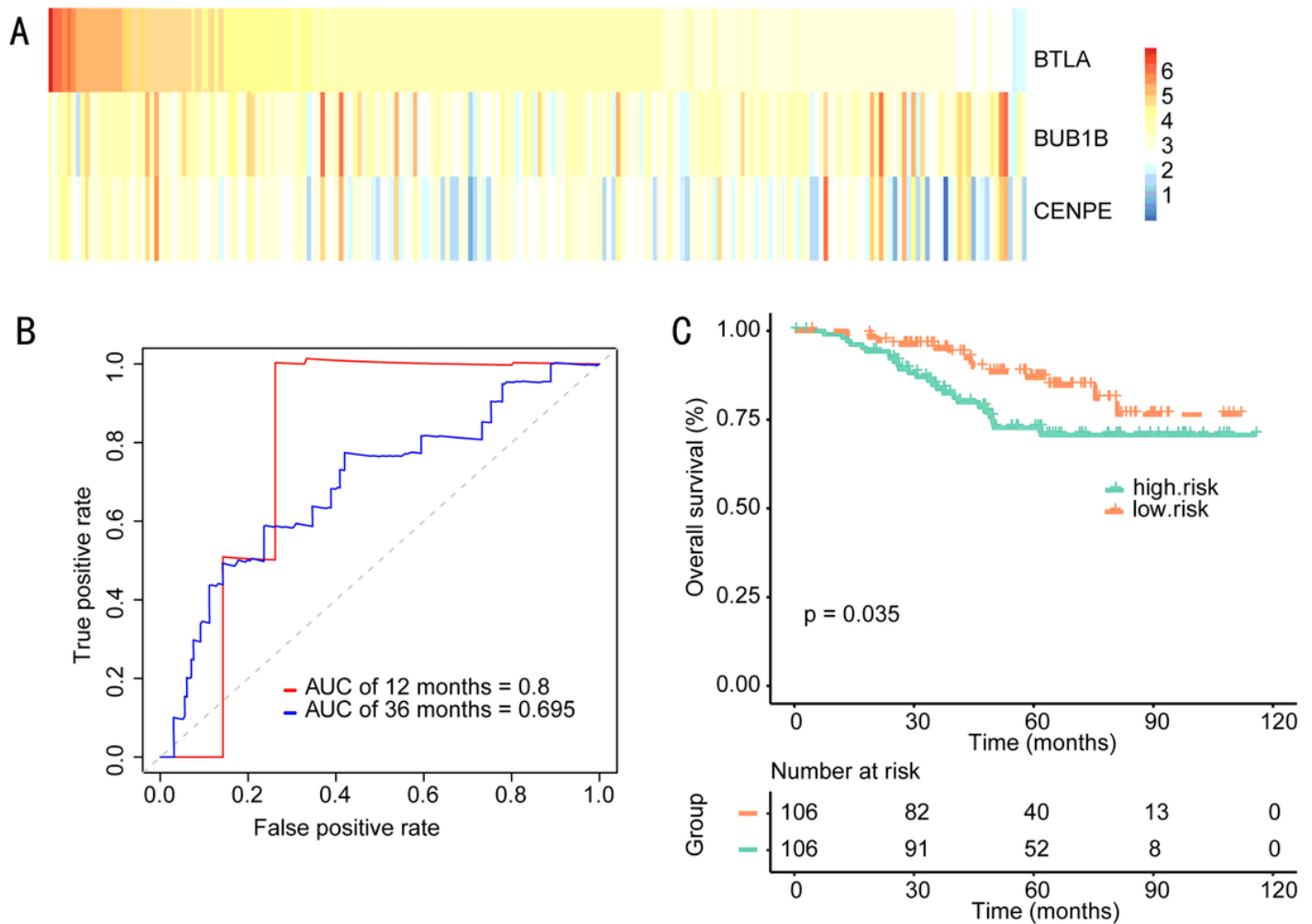


Figure 4

Validating the validity and reliability of the gene signature in four external datasets (GSE31210, GSE26939, GSE72094, and GSE11969). (A) Heat map of three gene expressions (BTLA, BUB1B and CENPE). (B) ROC curves of the gene signature at 12 months and 36 months. (C) Kaplan–Meier survival curves for OS in the high and low risk group and number of patients.

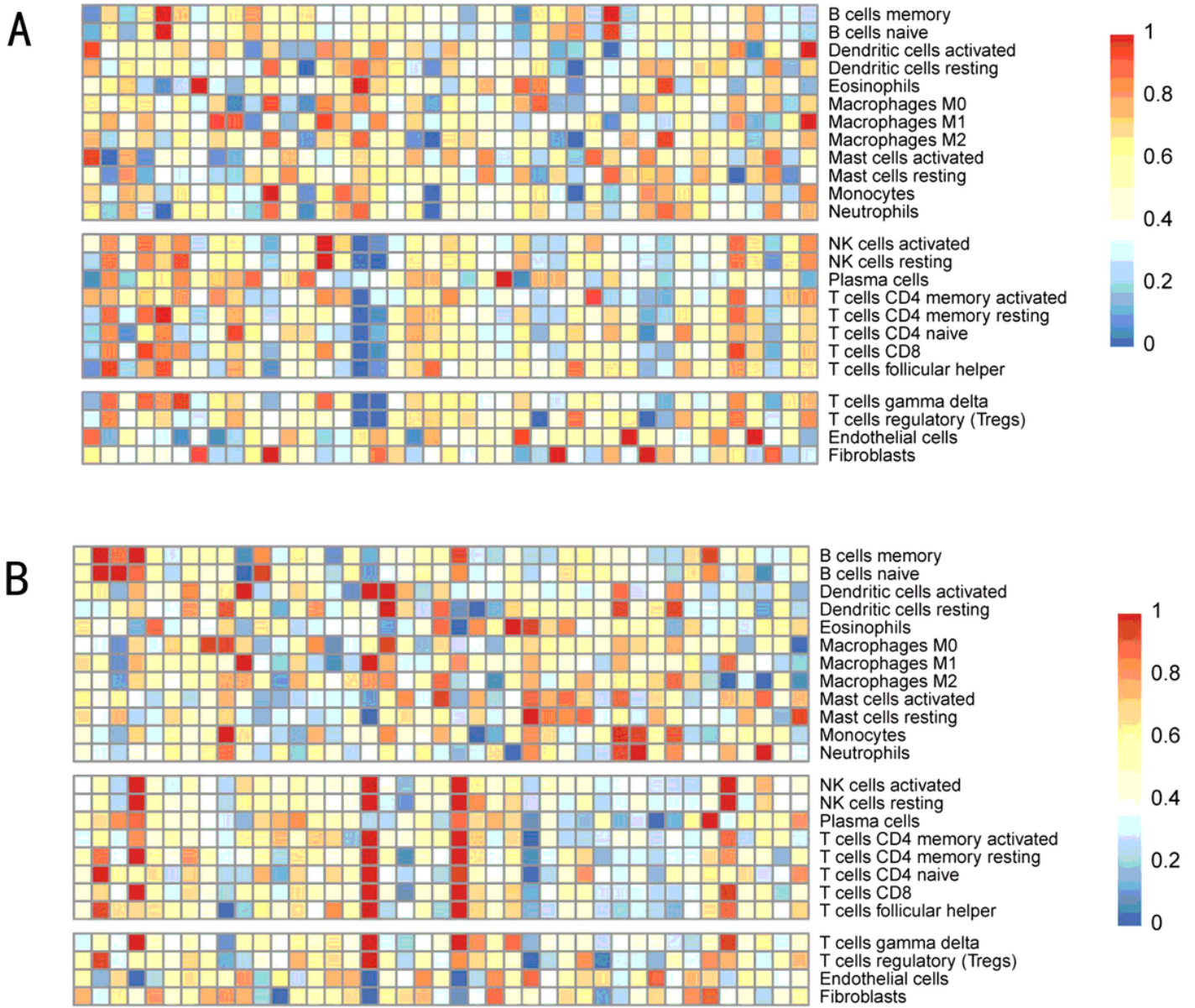


Figure 5

Estimating the abundance of immune cells infiltration in dataset GDC from TCGA. The abundance of 24 types immune cells infiltration in the low (A) and high risk group (B).